

## Measurement of thin film shape with a sinusoidal wavelength scanning interferometer using a white light source

Osami Sasaki, Hiroshi Ueno, and Takamasa Suzuki

Faculty of Engineering, Niigata University, 8050Ikarashi 2, Niigata-shi 950-2181, Japan

Fax 81-25-262-6747 E-mail: osami@eng.niigata-u.ac.jp

### ABSTRACT

A halogen lamp and an acousto-optic tunable filter are used to construct a sinusoidal wavelength-scanning interferometer with the scanning width of 210 nm. A linear wavelength-scanning with the scanning width of 220 nm is utilized to determine amplitudes of three different interference signals produced from multiple-reflection lights by front and rear surfaces of a thin film. Amplitudes of time-varying phases produced by a sinusoidal wavelength-scanning and constant phases in the interference signals are estimated by minimizing a difference between detected signals and theoretical ones. From the estimated values, the positions of the front and rear surface of the thin film with a thickness of about 460 nm are measured with an error less than 4 nm.

**Keywords:** interferometer, wavelength scanning, shape measurement, thin film

### 1. INTRODUCTION

It is required for the manufacturing process of devices such as semiconductors and liquid crystals displays that profiles of front and rear surfaces and thickness distribution of a thin film are measured with a high accuracy of a few nanometers. To achieve this three-dimensional measurement, white light interferometers and wavelength-scanning interferometers have been developed. In white light interferometers, the positions of the reflecting surfaces are determined by finding positions where the amplitude of the interference signal has a peak by scanning the optical path difference (OPD) [1]. In wavelength-scanning interferometers, changes of the interference signal according to the scanning of the wavelength are utilized for the thickness measurement. In the case of linear wavelength-scanning, the positions of the reflecting surfaces are determined by the peaks of the frequency spectrum of the interference signal [2]. When thickness of a film is very thin, the two peaks that provide the positions of the two surfaces of the film become too close to distinguish the two peaks. Therefore, this conventional idea of finding the peaks has a difficulty in measuring the positions of the two reflecting surfaces of a thin film. The other idea to overcome this difficulty is to estimate unknowns which are related to the two peaks by minimizing a difference between signals derived from the detected interference signal and theoretical ones. This signal processing is called signal fitting. The idea of the signal fitting was applied to the measurements reported in references [3-6]. Signals derived from the detected interference signal were spectral phase functions produced by an OPD-scanning in a white light interferometer [3] and by a linear wavelength-scanning [4, 5]. Measurable thickness of a thin film in these measurements is more than one micron. A white light interferometer using a signal fitting achieved the measurable thickness of less than one micron [7].

In this paper we propose a different method using a sinusoidal wavelength-scanning [6] compared with the methods in references [4,5]. The unique points in the sinusoidal wavelength-scanning are that the interference signal is a time-continuous signal and an exact wavelength-scanning with a larger scanning width is easily performed. These points enable us to extend the measurable thickness of a thin film to less than one micron.

Moreover a linear wavelength-scanning is also used to get initial values of the unknowns for the signal fitting. Using the sinusoidal wavelength-scanning between about 550 nm and 750 nm and estimating the values of unknowns contained in the interference signal, the positions of the front and rear surface of a thin film with a thickness of about 460 nm are measured with an error less than 4 nm.

## 2. SINUSOIDAL WAVELENGTH-SCANNING INTERFEROMETER

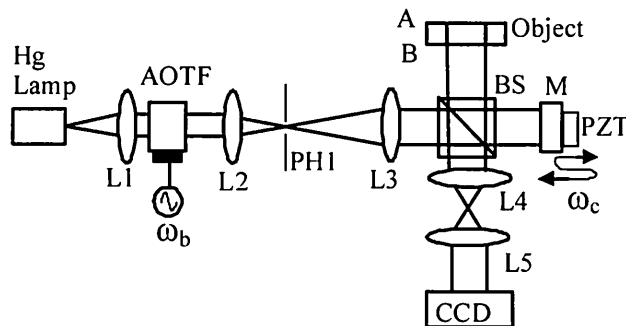


Fig. 1 Sinusoidal wavelength-scanning interferometer for measuring thickness and surface profiles of a thin film.

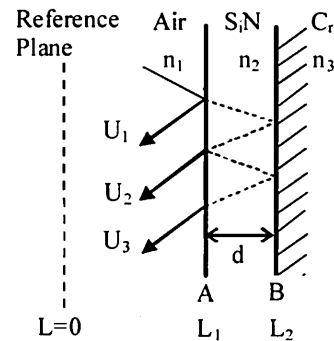


Fig. 2 Multiple reflections by a thin film.

Figure 1 shows an interferometer for measuring thickness and surface profiles of a thin film. The output light of a halogen (HG) lamp is collimated by lens L1 and incident on an acousto-optic tunable filter (AOTF). The wavelength of the first-order diffracted light from the AOTF is proportional to the frequency of the signal applied to an acoustical transducer in the AOTF. Modulating the frequency of the applied signal sinusoidally, the wavelength of the light from the AOTF is scanned as follows:

$$\lambda(t) = \lambda_0 + b \cos(\omega_b t), \quad (1)$$

where  $\lambda_0$  is the central wavelength. The intensity of the light source is also changed, and it is denoted by  $M(t)$ . The light is divided into an object light and a reference light by a beam splitter (BS). The reference light is sinusoidally phase modulated with a vibrating mirror M whose movement is a waveform of  $a \cos(\omega_c t + \theta)$ .

The object is a silicon nitride film coated on a chrome film as shown in Fig. 2, and the refractive index of air, silicon nitride, and chrome are denoted by  $n_1$ ,  $n_2$  and  $n_3$ , respectively. The film has two surfaces A and B, and multiple-reflection light from the two surfaces is defined by  $U_i$  ( $i=1, 2, 3, \dots$ ). The amplitudes of the interference signals produced by a reference light and the object light  $U_i$  are denoted by  $a_i$  ( $i=1, 2, 3, \dots$ ). The values of  $a_2$  and  $a_3$  are normalized by regarding the value of  $a_1$  to be unity. The interference signals produced by  $U_4$  are neglected under the assumption of the amplitude of  $a_4 \ll a_1$ . Although lights  $U_i$  ( $i=1, 2, 3$ ) interfere with each other to produce interference signals, these interference signals can be filtered out through Fourier transform of the interference signals because the reference light is sinusoidally phase modulated. The positions of two surfaces A and B are expressed by OPDs  $L_1$  and  $L_2$ . Among the detected interference signals the interference signals produced by interference between  $U_i$  ( $i=1, 2, 3$ ) and the reference light are expressed as

$$S(t) = M(t) \sum_i a_i \cos[Z_c \cos(\omega_c t + \theta) + Z_{bi} \cos(\omega_b t) + \alpha_i], \quad (i=1, 2, 3) \quad (2)$$

where

$$\begin{aligned} Z_c &= 4\pi a / \lambda_0, \quad Z_{bi} = 2\pi b L_i / \lambda_0^2, \quad \alpha_i = 2\pi L_i / \lambda_0, \quad (i=1, 2) \\ Z_{b3} &= Z_{b1} + 2(Z_{b2} - Z_{b1}), \quad \alpha_3 = \alpha_1 + 2(\alpha_2 - \alpha_1) + \pi. \end{aligned} \quad (3)$$

Putting  $\Phi_i = Z_{bi} \cos(\omega_b t) + \alpha_i$ , the interference signal  $S(t)$  is rewritten as

$$S(t) = M(t) A \cos[Z_c \cos(\omega_c t + \theta) + \Phi(t)], \quad (4)$$

where,

$$A \exp[j\Phi(t)] = \sum_i a_i \exp(j\Phi_i) \quad (i=1, 2, 3) \quad (5)$$

The intensity modulation  $M(t)$  is obtained by detecting the intensity of the reference light. The Fourier transform of  $S(t)/M(t)$  is denoted by  $F(\omega)$ . If the following conditions are satisfied,

$$\Im[A \sin\Phi(t)] = 0, \quad \Im[A \cos\Phi(t)] = 0, \quad |\omega| > \omega_c/2 \quad (6)$$

where  $\Im[y]$  is the Fourier transformation of  $y$ . The frequency components of  $F(\omega)$  in the regions of  $\omega_c/2 < \omega < 3\omega_c/2$  and  $3\omega_c/2 < \omega < 5\omega_c/2$  are designated by  $F_1(\omega)$  and  $F_2(\omega)$ , respectively. Then we have

$$\begin{aligned} F_1(\omega - \omega_c) &= -J_1(Z_c) \exp(j\theta) \Im[A \sin\Phi(t)], \\ F_2(\omega - 2\omega_c) &= -J_2(Z_c) \exp(j2\theta) \Im[A \cos\Phi(t)], \end{aligned} \quad (7)$$

where  $J_n(Z_c)$  is the  $n$ th-order Bessel function. The values of  $Z_c$  and  $\theta$  are measured by sinusoidal phase-modulation interferometry beforehand. Taking the inverse Fourier transform of  $-F_1(\omega - \omega_c)/J_1(Z_c) \exp(j\theta)$  and  $-F_2(\omega - 2\omega_c)/J_2(Z_c) \exp(j2\theta)$ , we obtain

$$\begin{aligned} A_s(t) &= A \sin\Phi(t) = \sum_i a_i \sin[Z_{bi} \cos(\omega_b t) + \alpha_i], \\ A_c(t) &= A \cos\Phi(t) = \sum_i a_i \cos[Z_{bi} \cos(\omega_b t) + \alpha_i]. \end{aligned} \quad (i=1, 2, 3) \quad (8)$$

When the absolute value of  $Z_{bi}$  increases, the frequency distributions of  $F_1(\omega)$  and  $F_2(\omega)$  have a wider band around  $\omega_c$  and  $2\omega_c$ , respectively, due to the terms of  $Z_{bi} \cos(\omega_b t)$ . Since the conditions given by Eq. (6) must be satisfied, maximum detectable value of  $|Z_{bi}|$  depends on the ratio of the  $\omega_c/\omega_b$ . In contrast, when the absolute value of  $Z_{bi}$  decrease, the magnitude of the spectra in  $F_1(\omega)$  and  $F_2(\omega)$  becomes so small that they can not be distinguished from noise. Therefore the absolute value of  $Z_{bi}$  must be between 1 rad and 12 rad at  $\omega_c = 32\omega_b$ .

The detected values of  $A_s(t_m)$  and  $A_c(t_m)$  are obtained from the detected interference signals at intervals of  $\Delta t$ , where  $t_m = m\Delta t$  and  $m$  is an integer. Using the detected values of  $A_s(t_m)$ ,  $A_c(t_m)$ , and known values of  $K_i = a_i/a_1$  ( $i=2, 3$ ), we define an error function

$$H = \sum_m \{ [\hat{A}_s(t_m) - A_s(t_m)]^2 + [\hat{A}_c(t_m) - A_c(t_m)]^2 \}, \quad (9)$$

where  $\hat{A}_s(t_m)$  and  $\hat{A}_c(t_m)$  are the estimated signals which contain unknowns of  $a_i$ ,  $Z_{bi}$ , and  $\alpha_i$  ( $i=1, 2$ ). The values of unknowns of  $a_i$ ,  $Z_{bi}$ , and  $\alpha_i$  are searched to minimize  $H$  by multidimensional nonlinear least-squares algorithm.

We obtain values of  $L_i$  from the values of  $Z_{bi}$  that is denoted by  $L_{zi}$ , and also obtain other values of  $L_i$  from the values of  $\alpha_i$  that is denoted by  $L_{\alpha i}$ . Since the measurement range of  $\alpha_i = 2\pi L_{\alpha i} / \lambda_0$  is limited  $-\pi$  to  $\pi$ , a value of  $L_{\alpha i}$  is limited to the range from  $-\lambda_0/2$  to  $\lambda_0/2$ . On the other hand, a value of  $Z_{bi} = 2\pi b L_{zi} / \lambda_0^2$  provides a rough value  $L_{zi}$  of  $L_i$ . To combine  $L_{zi}$  and  $L_{\alpha i}$ , the following equation is used:

$$m_{ci} = (L_{zi} - L_{\alpha i}) / \lambda_0. \quad (10)$$

If the measurement error  $\epsilon_{L_{zi}}$  in  $L_{zi}$  is smaller than  $\lambda_0/2$ , a fringe order  $m_i$  is obtained by rounding off  $m_{ci}$ . The suffixes of  $i=1$  and  $2$  in the  $L_{zi}$ ,  $L_{ai}$ ,  $m_{ci}$ , and  $m_i$  correspond to surface A and B, respectively. Then an OPD  $L_i$  longer than a wavelength is given by

$$L_i = m_i \lambda_0 + L_{ai}. \quad (11)$$

Since the measurement accuracy of  $L_{ai}$  is a few nanometers, an OPD over several ten micrometers can be measured with a high accuracy.

The positions  $P_1$  and  $P_2$  of the front and rear surfaces, respectively, are obtained from the estimated values as follows:

$$P_1 = (m_1 \lambda_0 + L_{a1})/2, \quad P_2 = P_1 + [m \lambda_0 + (L_{a2} - L_{a1})]/2n_2, \quad (12)$$

where  $m = m_2 - m_1$ . The thickness  $d$  is given by  $P_2 - P_1$ . Thus we can measure the thickness and the two surface profiles of the thin film.

### 3. ADJUSTMENTS AND MEASUREMENTS WITH A LINEAR WAVELENGTH-SCANNING

The values of  $a_2$  and  $a_3$  were determined by using a linear wavelength-scanning since their exact values were not known. When the linear wavelength-scanning width and an OPD is  $B_\lambda$  and  $L$ , respectively, the condition for the interference signal to have one cycle in the period of the wavelength-scanning is given approximately by  $B_\lambda = \lambda_0^2/L$ . In this case the Fourier transform of the interference signal has one frequency component. The optical path length corresponding to the distance of  $2d$  in Fig.2 is denoted  $L_{AB}$ . Since  $d = 470 \mu\text{m}$  and  $n_2 = 1.9$ ,  $L_{AB} = 1.8 \mu\text{m}$ . For  $\lambda_0 = 660 \text{ nm}$  and  $L = L_{AB} = 1.8 \mu\text{m}$ ,  $B_\lambda = \lambda_0^2/L = 250 \text{ nm}$ . An interference signal generated from the object lights  $U_i$  ( $i=1, 2, 3$ ) without the reference light was detected by blocking the reference light. The linear wavelength-scanning width was adjusted so that the Fourier transform of the interference signal had larger amplitude at a frequency of  $f_b$ . From this adjustment  $B_\lambda = 232 \text{ nm}$  was obtained.

Next the position of the reference mirror was adjusted so that the OPD  $L_1$  became zero by observing the interference signal. At  $L_1 = 0$  the amplitude of the interference signal becomes the smallest. After that the position of the reference mirror was moved by  $4L_{AB}/2 = 3.6 \mu\text{m}$  and the Fourier transform of the interference signal was obtained. The position of the reference mirror was adjusted so that the Fourier transform of the interference signal had smaller amplitude at the frequency of  $3f_b$ . The obtained amplitude of the Fourier transform is shown in Fig.3. Since the amplitudes of the frequencies  $4f_b$ ,  $5f_b$ , and  $6f_b$  correspond to the amplitudes of  $U_1$ ,  $U_2$ , and  $U_3$ , respectively, the values of  $K_i = a_i/a_1$  ( $i=2, 3$ ) were determined to be 1.6 and 0.2, respectively, from the results of Fig.3. At the same time the initial values of  $Z_{b1}$  and  $Z_{b2}$  were determined to be 3 rad and 6 rad, respectively, from the position of the reference mirror and the rough value of  $d$  at  $\lambda_0 = 660 \text{ nm}$  and  $b = 105 \text{ nm}$  with Eq.(3).

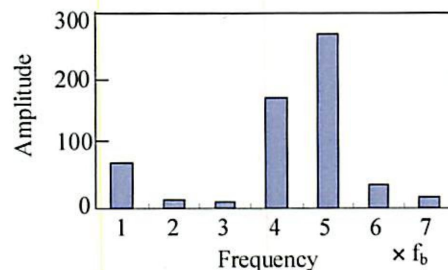


Fig. 3 Fourier transform of the interference signal by linear wavelength-scanning.

#### 4. EXPERIMENTS

While searching for the real values of the unknowns, the existences of numerous local minima was recognized. The conditions of the initial values were examined by computer simulations. The initial values move to the real values almost certainly when differences between the initial values and the real values are within the following values: about 2rad for  $Z_{b1}$  and  $Z_{b2}$ , about 1.5rad for  $\alpha_1$  and  $\alpha_2$ , and about 50% accuracy for  $a_1$ . However if one of these condition for the differences is not satisfied, the initial values do not always reach the global minimum. Good initial values are required to reach the global minimum in a short time. The initial values of  $Z_{b1}$  and  $Z_{b2}$  obtained in the above section satisfy the above difference less than 2rad. On the other hand the initial values of  $\alpha_1$  and  $\alpha_2$  can not be determined from the detected signals. Therefore the initial value of  $\alpha_1$  is given at intervals of 1.0 rad in the range from  $-\pi$  to  $\pi$  rad for the initial value of  $\alpha_2=0$ . When a global minimum can not be obtained, the initial value of  $\alpha_2$  is changed by 1.0 rad and the search is repeated again. Considering all combinations of  $\alpha_1$  and  $\alpha_2$ , the search becomes successful at most after 36 repetitions. The values estimated first at one measuring point are used as the initial values of the adjacent measuring points, because the difference in real values of  $\alpha_1$  and  $\alpha_2$  between the adjacent measuring points is within  $\pi/2$  to detect the interference signal with a sufficient amplitude.

We constructed the interferometer shown in Fig. 1. The central wavelength  $\lambda_0$  and the wavelength-scanning width  $2b$  were 660.2 nm and 210 nm, respectively. The scanning frequency of  $\omega_b/2\pi$  was 16.3 Hz and the phase modulating frequency of  $\omega_c/2\pi$  was  $32(\omega_b/2\pi)=521.6$  Hz. A two-dimensional CCD image sensor was used to detect the interference signals. Lenses L4 and L5 formed an image of the object on the CCD image sensor with magnification of 1/3. Number of the measuring point was  $60 \times 30$  in a region of  $3.6 \text{ mm} \times 1.8 \text{ mm}$  on the object surfaces along the x and y axes, respectively. Positions of the pixels of the CCD image sensor are denoted by  $I_x$  and  $I_y$ , respectively. Intervals of the measuring points were  $\Delta x=30 \mu\text{m}$  and  $\Delta y=30 \mu\text{m}$ .

First, values of unknowns  $Z_{b1}$ ,  $Z_{b2}$ ,  $\alpha_1$  and  $\alpha_2$  were estimated at a measuring point of  $I_x=1$  and  $I_y=1$  by minimizing the error function given by Eq. (9). The results are shown at Table 1, where the four cases of different initial values (IV) are presented. Exact estimated values (EV) are obtained at Case 1 and 3. Figure 4 shows the estimated signal and the detected signal at Case1. The estimated values at a measuring point were used as initial values of the adjacent measuring points. By combining  $L_{zi}$  and  $L_{\alpha i}$  with Eq. (10), the values of  $m_{C1}$  and  $m_{C2}$  for the front and rear surface, respectively, were obtained as shown in Fig.5. Since the front and rear surface changed smoothly, it was clear that fringe order  $m_1$  and  $m_2$  were constant values. It was decided that fringe order  $m_1$  and  $m_2$  were 6 and 9, respectively, from Fig.5. Figure 6 shows the positions  $P_1$  and  $P_2$  of the front and rear surface calculated with Eq. (12). Figure 7 shows the thickness distribution calculated from  $P_2-P_1$ . It was made clear by repeating the measurement three times that the measurement repeatability was less than 4 nm.

**Table 1** Estimated values (EV) and initial values (IV) at one measuring point.

| Case |    | a    | $Z_{b1}$ (rad) | $Z_{b2}$ (rad) | $\alpha_1$ (rad) | $\alpha_2$ (rad) | H   |
|------|----|------|----------------|----------------|------------------|------------------|-----|
| 1    | IV | 1.0  | 3              | 6              | 1                | -2               | 42  |
|      | EV | 0.94 | 3.21           | 6.33           | -1.29            | 1.72             | 7   |
| 2    | IV | 1.0  | 3              | 6              | -1               | 0                | 27  |
|      | EV | 0.46 | 4.50           | 7.15           | 3.14             | 1.65             | 15  |
| 3    | IV | 1.0  | 3              | 6              | 2                | -1               | 46  |
|      | EV | 0.94 | 3.21           | 6.33           | -1.29            | 1.72             | 7   |
| 4    | IV | 1.0  | 3              | 6              | 1                | 1                | 317 |
|      | EV | 0.2  | 4.5            | 8.0            | 3.14             | -3.14            | 17  |

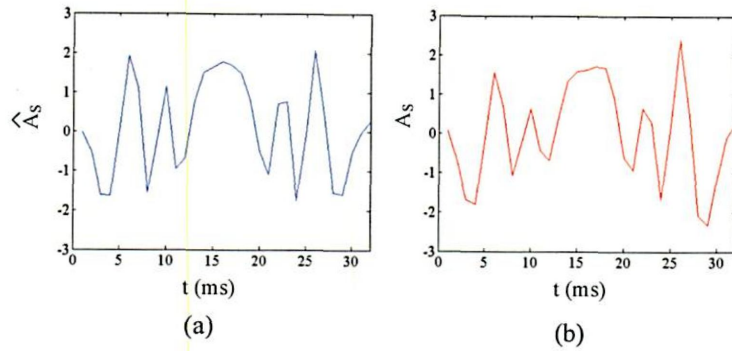


Fig.4 (a) Estimated signal  $\hat{A}_S$  and (b) detected signal  $A_S$ .

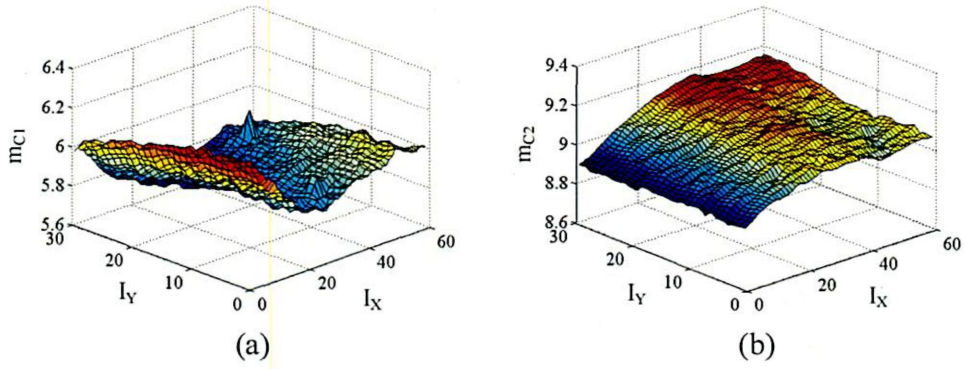


Fig.5 Measured results of (a)  $m_{C1}$  and (b)  $m_{C2}$ .

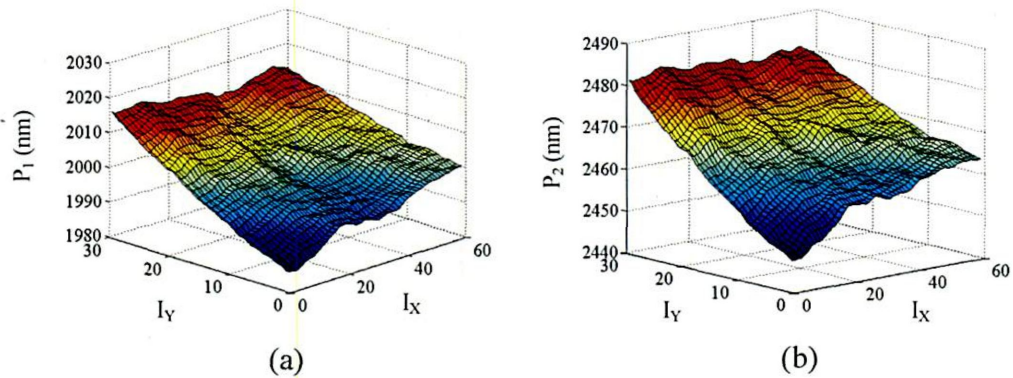


Fig.6 Measured results of (a)  $P_1$  and (b)  $P_2$ .

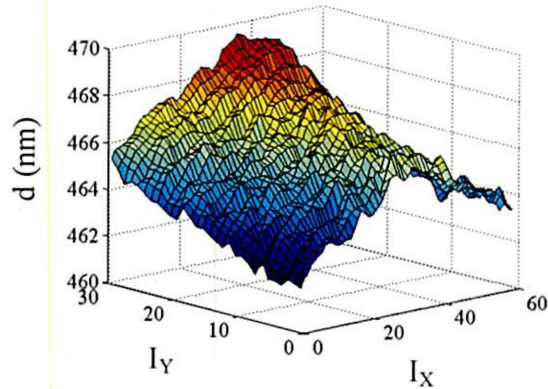


Fig.7 Measured thickness distribution  $d$  of  $P_2 - P_1$ .

## 5. CONCLUSION

The halogen lamp and the acousto-optic tunable filter (AOTF) were used to obtain a large wavelength-scanning width. The linear wavelength-scanning with the scanning width of 230 nm was utilized to determine the amplitudes of the three different interference signals produced from multiple-reflection lights by the front and rear surfaces. The values of the phase modulation  $Z_{bi}$  produced by the sinusoidal wavelength-scanning with the scanning width of 210 nm and the constant phase  $\alpha_i$  ( $i=1,2$ ) were estimated by minimizing the difference between the detected signals and theoretical ones. From the estimated values, the positions of the front and rear surfaces of the thin film with a thickness of about 460 nm were measured with an error less than 4 nm.

## REFERENCES

1. H. Maruyama, S. Inoue, T. Mitsuyama, M Ohmi and M Haruna, "Low-coherence interferometer system for the simultaneous measurement of refractive index and thickness," *Appl. Opt.* 41, 1315-1322 (2002).
2. T. Funaba, N. Tanno and H. Ito, "Multimode-laser reflectometer with a multichannel wavelength detector and its application," *Appl. Opt.* 36, 8919-8928 (1997).
3. S. W. Kim and G. H. Kim, "Thickness-profile measurement of transparent thin-film layers by white-light scanning interferometry," *Appl. Opt.* 38, 5968-5973 (1999).
4. D. Kim, S. Kim, H. J. Kong and Y. Lee, "Measurement of the thickness profile of a transparent thin film deposited upon a pattern structure with an acousto-optic tunable filter," *Opt. Lett.* 27, 1893-1895 (2002).
5. D. Kim, S. Kim, "Direct spectral phase function calculation for dispersive interferometric thickness profilometry," *Opt. Express.* 12, 5117-5124 (2004).
6. H. Akiyama, O. Sasaki, and T. Suzuki, "Sinusoidal wavelength-scanning interferometer using an acousto-optic tunable filter for measurement of thickness and surface profile of a thin film," *Opt. Express* 13, 10066-10074 (2005).
7. K. Kitagawa, "Recent trends in white-light interferometry," *Proc. SPIE* 6382, 638201 (2006).